Basic Science

The effect of implant size and device keel on vertebral compression properties in lumbar total disc replacement

Joshua D. Auerbach, MD[a,b,*], Carrie M. Ballester, MSE[b], Frank Hammond, MSE[b],
Ehren T. Carine, BS[b], Richard A. Balderston, MD[c], Dawn M. Elliott, PhD[b]

[a]Department of Orthopaedics, Bronx-Lebanon Hospital Center, Albert Einstein College of Medicine, Bronx, NY 10457, USA
[b]Department of Orthopaedic Surgery, McKay Orthopaedic Research Laboratory, University of Pennsylvania, Philadelphia, PA 19104, USA
[c]Booth, Bartolozzi, and Balderston Orthopaedics, Pennsylvania Hospital, Philadelphia, PA 19104, USA

Abstract

BACKGROUND CONTEXT: Vertebral end plate support is necessary for successful lumbar total disc replacement (TDR) surgery. Failure to achieve anterior column support as a result of lumbar TDR device undersizing could lead to implant subsidence and fracture.

PURPOSE: The purpose of the study was to examine the compressive biomechanical behavior of the vertebral end plate with varying sizes of disc replacement implants.

STUDY DESIGN: The study design comprises a biomechanical investigation using a human cadaveric lumbar spine model.

METHODS: Fifty-six vertebrae with intact posterior elements were prepared from 13 fresh frozen lumbar spines. Peripheral quantitative computed tomography was performed to assess regional bone density. Vertebrae were potted and subjected to nondestructive compression testing with a small, medium, and large custom-made implants with the footplate geometry of the ProDisc-L TDR (Synthes Spine, West Chester, PA, USA) system and having no keel. Failure testing was performed using the ProDisc-L implant with an intact keel. Pressure sensor film was used to assess contact pressure and distribution.

RESULTS: There was a linear correlation between percent coverage of the end plate and implant-end plate stiffness (p=.0001) and an inverse correlation with displacement (p=.01). The difference in implant-end plate stiffness between small-medium, medium-large, and small-large implants was 10.5% (p=.03), 10.2% (p=.02), and 19.6% (p<.0001), respectively. Failure analysis revealed similar trends for implant sizing, but only bone density was found to significantly correlate with failure properties (r=0.76, p<.0001). There was a significant reduction in implant-end plate stiffness of 18% when the keel was intact compared to without the keel (range 6–27%, p=.0008). Pressure film analysis revealed that the implant was loaded peripherally and did not have central contact during nondestructive loading. There was a trend toward greater contact pressure with the small implant when compared with the medium implant (p=.06) and the large implant (p=.06).

CONCLUSIONS: Although larger implants reduce end plate displacement, increase apparent implant-end plate stiffness, increase the implant-end plate contact area, and decrease the peak contact pressures, low bone density reduces failure properties. The keel introduces a reduction in stiffness to the implant-end plate interface, the clinical significance of which is currently unknown. © 2010 Elsevier Inc. All rights reserved.

Keywords: Lumbar total disc arthroplasty; End plate; Compression; Mechanics; Keel

* Corresponding author. Department of Orthopaedics, Bronx-Lebanon Hospital Center, Albert Einstein College of Medicine, 1650 Grand Concourse, 7th Floor, Bronx, NY 10457, USA. Tel.: (609)-202 6173.

E-mail address: auerspine@gmail.com (J.D. Auerbach)

Introduction

The clinical efficacy of lumbar total disc replacement (TDR) compared with spinal fusion for the treatment of degenerative disc disease has been shown in several recent clinical trials [1–5]. Although the outcome of lumbar TDR is likely dependent on multiple patient- and surgeon-related factors, there is evidence to suggest that implant sizing is a critical component for success, and that failure to do so could predispose to significant morbidity [2,6–11]. Failure to achieve adequate anterior column support as a result of lumbar TDR device undersizing could lead to implant subsidence and fracture [6,8,9,12,13]. Although long-term follow-up will be needed to fully appreciate the spectrum of complications that may result from subsidence with TDR, recent studies from both TDR and fusion cage literature have shown that kyphotic deformity, neural element compromise, great vessel compression, small bowel obstruction, pain, wear debris leading to osteolysis, and the need for revision surgery are some of the sequelae that may develop [6,8,9,11,12,14,15]. Subsidence depends, in part, on the stiffness and strength of the implant-end plate interface, and factors that influence this interface include bone mineral density, amount of cartilaginous end plate removal during surgery, anteroposterior position of the implant on the vertebral end plate (ie, variable regional bone strength), implant shape, and implant size [15–18].

The effect of fusion cage implant size has been evaluated as a factor in implant-end plate mechanics. In a cadaveric model, Tan et al. [18] demonstrated significantly higher failure loads and strength with larger fusion cage indenters. Similarly, Lowe et al. [17] reported that larger diameter cages facilitated a more efficient transfer of force toward the stronger posterolateral region of the end plate and, therefore, provided the greatest resistance to subsidence. There are, however, several technical aspects of the TDR procedure that affect the implant-end plate interface differently than that seen with fusion: 1) retention of the bony end plate, removing only the cartilaginous end plate [6]; 2) no attempt at arthrodesis between the end plate and the implant; and 3) a keeled implant is common, which may effect the mechanical integrity of the end plate leading to vertebral fracture [7,19]. Considering these factors, it is clear that end plate preparation, sizing goals, implant size and geometry, and interface mechanics may be different in lumbar TDR compared with fusion. Consequently, the conclusions drawn from studies of fusion cage devices may not be the same in evaluating the implant-end plate interface in lumbar TDR [5].

The objective of the present study was to examine the compressive biomechanical behavior of the vertebral end plate with varying sizes of TDR implants. We hypothesized the following: there will be a relationship between the proportion of end plate that is covered by the implant (percent coverage) with the compressive biomechanical properties of displacement, stiffness, contact pressure, and failure load; bone density will correlate with implant-end plate mechanics; and the keel of the TDR implant will significantly alter the compressive biomechanics.

Methods

Study design

The study was performed with two arms: nondestructive and failure mechanical testing using an implant with the inferior footprint geometry of the ProDisc-L TDR (Synthes Spine, West Chester, PA, USA). First, nondestructive testing was performed using repeated tests of three implant sizes. Because repeated testing was performed, low loads were applied, and repeatability was confirmed. In the nondestructive testing, each specimen was tested with the implant keels removed (Fig. 1, left). Removal of the keel was performed to evaluate the mechanics of the implant-end plate interface without the effects of the keel and potential damage from inserting and removing the keel during repeated testing. Second, failure testing was performed using the ProDisc-L implant with the keel intact (Fig. 1, right). An intact TDR implant was used to more closely represent the physiological loading for determination of failure loads and displacements and to determine the effect of the keel by comparing the low load behavior with nondestructive behavior.

Imaging and specimen preparation

Thirteen fresh frozen lumbar spines (ages 27–77 years, average 61.6 years), which had a total of n=62 lumbar levels L1 through L5, were acquired under an approved institutional review board protocol. Intact spines were first assessed for structural deformities with anteroposterior and lateral radiographs. Levels with fractures, end plate irregularities (i.e., Schmorl's node), or tumors were removed (n=6), leaving a total of 56 intact specimens included in
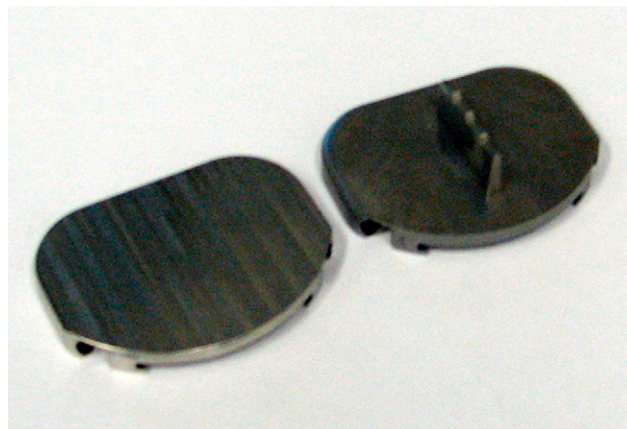

Fig. 1. Image of ProDisc-L total disc replacement implant geometry with (Left) customized with keel removed for nondestructive testing and (Right) keel intact for failure testing.

the study. Peripheral quantitative computed tomography (XCT2000; Stratec Medizintechnik, Pforzheim, Germany) was performed on each vertebral level while the entire lumbar spine was still intact. Three evenly spaced axial slices through the vertebral body were acquired and for each slice trabecular bone density within a 10-mm circular region of interest was quantified using customized digital software program (Fig. 2). Bone density for the each vertebral body was defined as the average from each of the three axial slices.

After imaging, lumbar specimens between L1 and L5 were dissected to remove all surrounding soft tissues. Posterior elements, which contribute toward vertebral compression mechanics, were kept intact and had no evidence of pars fractures, pedicle fractures, prior laminectomies, or spina bifida occulta. The superior end plate (the end plate in contact with the TDR implant) was prepared by sharp dissection of the disc with a scalpel, followed by removal of the remaining disc until the cartilaginous end plate was exposed. A curette was then used to remove the remaining cartilaginous end plate while taking care to remove only the cartilaginous end plate, leaving the bony end plate intact. This end plate preparation was performed according to the method prescribed by a spine surgeon with extensive experience in lumbar disc replacement surgery. The inferior end plate preparation consisted of removal of disc and cartilaginous end plate using a scalpel and curette.

The specimen was then potted by placing the inferior body centrally within a plastic cylinder and filling the cylinder with polymethylmethacrylate to cover the inferior 2 to 3 mm of the vertebral body (Fig. 3). Care was taken to ensure that the pedicles did not come into contact with the cylinder. A level was used to ensure a flat, even surface at the superior end plate. Anteroposterior dimensions taken at the vertebral body sagittal midline and mediolateral end plate dimensions taken in the coronal plane vertebral body midline were measured three times using a digital caliper by a single observer, and the average value was used.

The percent coverage for each specimen and each implant size was calculated as the end plate area divided by the implant area (for implants, the areas were small=567, medium=738, and large=924 mm^2). The end plate surface area (A) was approximated by the area of an ellipse, A=π (anteroposterior radius) (mediolateral radius) as previously described [20–22]. In some cases, the implant was larger than the diameter of the body and "overhanging" the cortical rim. In these cases, the percent coverage was designated at a maximum of 100%. After dimensional measurement, the specimen was stored in a −20°C freezer until mechanical testing.

Mechanical testing

Before mechanical testing, specimens were removed from the freezer and thawed at room temperature. Each specimen first underwent nondestructive compression testing with small, medium, and large custom-made implants with the footprint geometry of the ProDisc-L (Synthes Spine, West Chester, PA, USA), but without the inferior keel (medium and large size ProDisc-L implants are commercially available; the small size implant is not currently available for clinical use). The order of nondestructive testing was randomized. Each specimen was placed under the indenter of the Instron 8874 (Instron Corporation, Canton, MA, USA) with the superior end plate oriented parallel to the horizontal plane, and the indenter placed centrally over the middle of the cancellous bone. A 0.48 to 2.41 MPa range pressure sensitive film (Fujifilm PressureX; Sensor Products, Inc., Madison, NJ, USA) was interposed between the implant and the end plate.

An initial preload of 50 N was applied at a rate of 0.2 mm/s and held for 60 seconds. After preload, a slow ramp
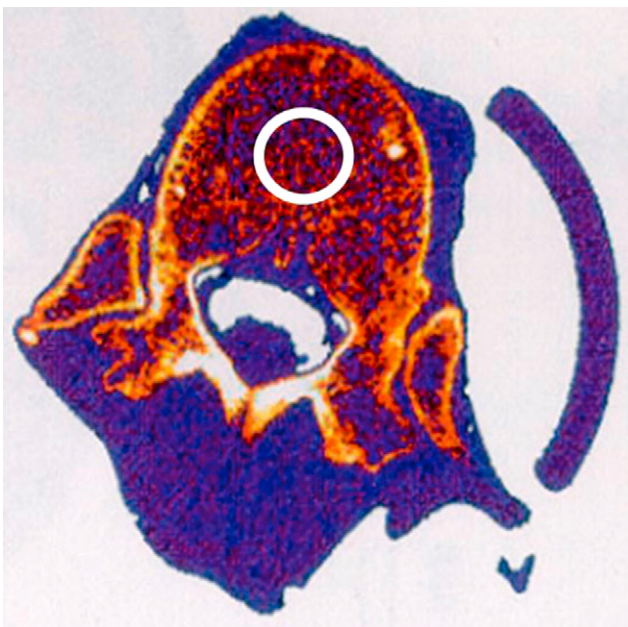

Fig. 2. Representative peripheral quantitative computed tomography scan of vertebral specimen. A 10-mm diameter circular region of interest of trabecular bone was evaluated for each specimen to determine bone density.
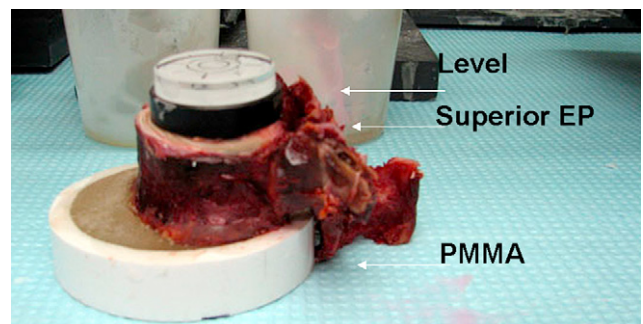

Fig. 3. Vertebral bodies were dissected and potted in polymethylmethacrylate using a level to keep the end plate surface flat.

was applied at the same rate until 400 N was reached. This low load was selected to prevent damage to the specimen and was based on previous studies of fusion implants [16,18]. After each test, the sample was unloaded and refrozen until repeated testing was performed. Twenty-four hours before the next testing session, the specimen was removed from the freezer and placed into a refrigerator for thawing. A subset of samples (n=15) that had been randomized to test with the small-sized implant first, followed by large and then medium implant, were retested with the small implant to confirm that repeated testing did not damage or alter the implant-end plate compression properties.

After completing the nondestructive testing, failure testing was performed once on each specimen using one implant size that was randomly assigned. The testing protocol was identical to that described above for nondestructive testing, except a ProDisc-L implant with an intact keel (Fig. 1, right) was used and the specimen was tested to failure rather than limited to 400 N load. The test was stopped when fracture had occurred or the load-displacement curve dropped.

Data analysis

The load-displacement response of each compression mechanical test was analyzed as follows. Stiffness was calculated using a linear regression of the load-displacement data between 200 and 400 N compression. Displacement at 400 N was recorded because the displacement of the implant into the end plate is a clinically significant indication of subsidence. For the failure testing, failure was defined as the maximum load in the load-displacement response. In those instances where the load-displacement response exhibited an early drop or a break in the curve, these were not recorded as max loads as long as the load continued to rise over the subsequent 0.5 mm displacement [23]. Additionally, the load at 2 mm displacement was recorded to represent subsidence.

A subset of pressure sensitive films (n=4) that had completed testing for all three implant sizes were scanned, digitized using custom software (Sensor Products, Inc., Madison, NJ, USA), and analyzed to assess contact pressures and distribution differences among the implant sizes.

Statistical analysis

The effect of the percent coverage, bone density, and other factors, such as level and age on the mechanical test parameters was evaluated. The mechanical test parameters considered were stiffness and displacement at 400 N load for all nondestructive and failure tests. Additionally, load at 2 mm displacement and maximum load were considered only for failure tests. The data were analyzed in two ways: groups were compared according to implant size (S, M, L) and individual specimens were analyzed according to continuous variable parameters (bone density and percent coverage).

To determine which factors, such as percent coverage, density, age, and level were linearly associated with mechanical parameters, the PROC MIXED procedure in SAS (SAS Institute, Inc., Cary, NC, USA) was used to account for the repeated measurement nature of the data. Because repeated measurements within patients may be correlated, this procedure allows one to model this "correlation structure," commonly referred to as a covariance pattern. This will allow for improved estimates of the standard errors of measurement, and therefore more powerful tests. There are a number of various covariance structures to choose from and here "compound symmetry" for correlations that are constant for any two points in time was chosen.

To quantify the effects of the keel on end plate compression mechanics, for each specimen, the stiffness calculated without the keel (nondestructive test) was compared with the stiffness calculated with the keel (destructive test) for the same implant size. Correlations were estimated by the Hamlett method, also incorporating PROC MIXED for repeated measures.

Results

The average percent coverage of the small, medium, and large implants was 38%, 50%, and 62%, respectively. The percent coverage was dependent on level and decreased at the lower levels, where the vertebral body area is larger.

Nondestructive results

After correcting for age, level, bone density, and gender, there was a linear correlation between percent coverage and stiffness (r=0.18, p=.0001). There was also an inverse correlation between percent coverage and displacement at 400 N (r=−0.10, p=.01). Therefore, stiffness significantly increased as implant size progressed from smaller to larger (Fig. 4, left). Likewise, displacement significantly decreased as implant size progresses from smaller to larger (Fig. 4, right). The difference in stiffness between small-medium, medium-large, and small-large implants was 10.5% (p=.03), 10.2% (p=.02), and 19.6% (p<.0001), respectively. The difference in displacement between small-medium, medium-large, and small-large implants was 15.0% (p=.0066), 2.6% (p=.69), and 17.2% (p=.0026). Bone density also significantly correlated with end plate stiffness (r=−0.25, p=.0003); however, bone density was not significantly correlated with displacement at 400 N (p=.26).

Repeatability testing confirmed that damage did not occur because of repeated implant mechanical testing. The median stiffness for the small implant during the first test was 723 N/mm and in the final test was 725 N/mm, with a median difference between testing sessions of 8%.

†: denotes significant differences vs small (p<0.05)
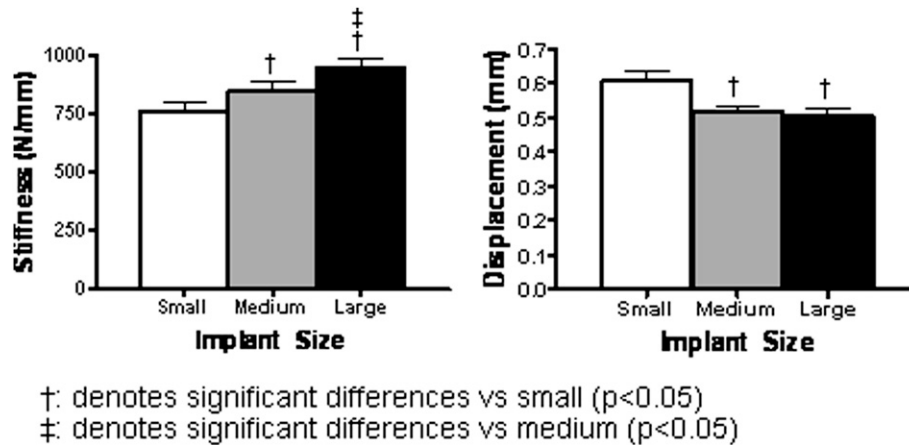‡: denotes significant differences vs medium (p<0.05)

Fig. 4. (Left) Stiffness at the implant-end plate interface increased significantly with increasing implant size. (Right) Displacement at 400-N compression decreased with increasing implant size.

This was not statistically different based on a paired *t* test, p=.49 using the Wilcoxon signed-rank test.

Fuji film analysis revealed that the implants were loaded peripherally and did not have central contact under nondestructive loads (Fig. 5, left). Larger implants also had increased end plate contact area with corresponding decreased contact pressures (Fig. 5, right). Although limited by small number of samples (n=4), there was a trend toward greater contact pressure with the small implant when compared with the medium implant (p=.06) and the large implant (p=.06), although there was no difference between the medium and the large implants (p=.7).

Failure results

In contrast to the nondestructive results, after correcting for age, level, bone density, and gender, there was no correlation between percent coverage and failure load (p=.3) or load at 2 mm displacement (p=.4). However, bone density was significantly correlated with failure properties. Linear regression analysis revealed that lower bone density significantly correlated with load at failure (r=0.76, p<.0001) and load required to produce 2 mm displacement (r=0.75, p<.0001). The failure load was 1961±937, 2624±1423, and 3087±1454 N for the small, medium, and large implants, respectively. The load at 2 mm displacement was 1499±775, 1900±1278, and 1959±813 N for the small, medium, and large implants, respectively. Although these followed the same trends as the nondestructive testing (Fig. 4), they were not significantly significant between implant sizes.

Effect of the keel

The stiffness calculated between 200 and 400 N from the nondestructive testing (no keel) and the failure testing (with keel) were compared to determine the effect of the keel on implant-end plate mechanics. After controlling for other variables, including percent coverage, bone density, age,

level, and gender, linear regression analysis revealed that on average the keel imparts a significant reduction in end plate stiffness of 18% (range: 6–27%, p=.0008). For the small implant, the keel decreased the stiffness by 6% (p=.41). In the medium and large implant groups, however, end plate stiffness decreased with the keel by 19% (p=.0043) and 26% (p=.0015), respectively.

Discussion

Lumbar TDR has shown equivocal or superior clinical results to spinal fusion in the treatment of degenerative disc disease [1–5,24]. The main impetus for TDR and other motion-preserving alternatives to fusion is the biomechanical advantage afforded by TDR, which theoretically protects the adjacent level from excessive stresses and adjacent segment degeneration requiring further surgery [25–35]. Although the clinical utility of lumbar TDR will continue to be debated [36,37], there is universal agreement that proper implantation technique and sizing are of critical importance to optimize device performance and clinical outcome [2,6–9,11,12,19,38]. Undersized arthroplasty devices may subject the central portion of the vertebral body to higher stresses and increase the risk for implant subsidence. Several studies have cited implant undersizing as the reason for subsidence and migration [6,8,9,12,13]. Although the true incidence of clinically relevant TDR device subsidence and failure is not known, it is likely that the proportion of current TDR patients who will ultimately develop subsidence or end plate fractures will increase, however, as this predominantly younger TDR population ages and experiences progressive bone loss and osteoporosis.

Biomechanical studies that have evaluated the mechanical effects of interbody fusion device shape, positioning, and size have shown that achieving peripheral rim fit on the stronger end plate regions are critical in minimizing the risk for subsidence [17,18,39,40]. Interbody fusion
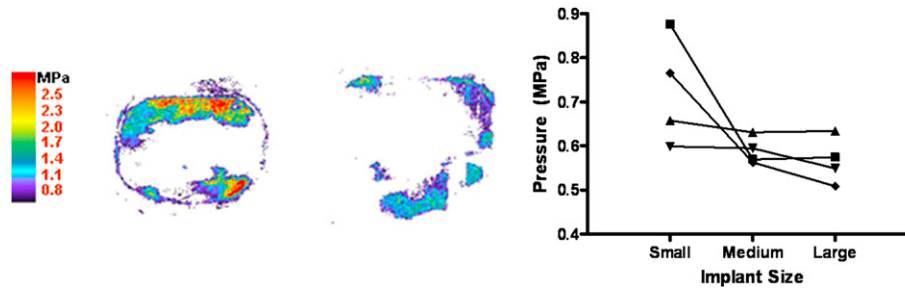
Fig. 5. Pressure film results. (Left) Representative small and large implant. (Right) Changes in average pressure with implant size.

devices often have roughened edges and unique shapes to maximize contact area and are designed to facilitate bony remodeling and fusion, which if achieved, will strengthen the bone-implant interface over time. The biomechanical environment in TDR, however, contains several unique aspects that make it different from that of a fusion. In TDR, only the cartilaginous end plate is removed (keeping the underlying bony end plate intact) to provide a bony buttress for the device footplate to rest on [1,6,40]. Although there is some expected bony ingrowth as a result of the plasma pore titanium coating with ProDisc-L, there is minimal bony remodeling and no intended fusion at the bone-implant interface. For these reasons, therefore, the initial bony support from the end plate and apophyseal rim in TDR is even more critical in the prevention of device subsidence. Most importantly, many TDR devices contain a keel, which penetrates the upper and lower end plates of the vertebrae, the path for which is generated by a chisel. Such a construct has the potential for serious end plate mechanical alterations, which to date have not been quantified.

Nondestructive analysis

The results of our study highlight that proper implant sizing may prevent subsidence by improving the initial implant-bone interface. By placing a larger implant, the implant rim rests on a stiffer, more peripheral region of the vertebral end plate, which can provide more mechanical support when compared with more central trabecular bone. With increasing implant size, the end plate stiffness significantly increased. Similarly, implant displacement was inversely correlated with implant size. Bone density had a significant correlation with end plate stiffness (statistically significant). Under relatively low loads (400 N), therefore, implant sizing has biomechanical effects on end plate mechanics. Significant differences were found under loads, which correspond to lying in the supine position. It could be expected that under loads corresponding to normal daily activities, which could be as much as fivefold higher, even more dramatic differences would be detected.

Pressure distribution analysis revealed that the implant is edge-loaded under compressive loads and that the central portion of the vertebral body may not be subjected to any relevant loads. Total disc replacement implants with a flat footplate, therefore, likely do not subject the weaker central bone under simulated physiologic compressive loads. It is unclear if the TDR implant undergoes some initial "settling" early on (<2 mm displacement), as described by Siepe et al. [41], which may actually represent bony remodeling around the flat edges of the implant and which does not appear to progress or cause symptoms. Because our study was a cadaveric model, it was not possible to simulate physiologic settling. It is possible, therefore, that end plate remodeling or minor settling may place the central portion of the vertebral body in contact with the footplate, which may help redistribute forces or, alternatively, load the weaker central bone. Although using a flat device footplate and avoiding loading the central vertebral body bone may reduce the risk for central depression or fracture, the majority of the contact area and pressure distribution are accounted for by the rim-loading edges of the implant. With the larger implant, there is a greater distribution of contact area and a trend toward reduced peak contract pressures (Fig. 5, left).

Failure analysis

Similar to the nondestructive testing, our results reveal that larger devices tended to have greater loads to failure and required greater loads to produce 2 mm of vertical displacement. Because of the variability of the data, however, these differences were not significant. This was not unexpected given the broad spectrum of ages, values for bone density, and vertebral levels tested. Bone density was the only factor that showed significant correlation with failure testing properties (max load at failure and load required to produce 2-mm vertical displacement). Other studies have shown that bone density is the critical component to determine the compressive strength of the vertebral body. Kayanja et al. [42] recently showed that when comparing nonaugmented versus augmented vertebral bodies with polymethylmethacrylate, the only factor that predicted failure loads was bone density. Although the percent end plate coverage by the implant is a predictor of end plate stiffness and risk for subsidence during nondestructive testing (400 N), perhaps these subfailure loads do not subject the underlying

trabecular bone to significant stresses. With increasing compressive loads, however, the underlying trabecular bone is called on to support the device footplate.

It is currently not known if nondestructive (subfailure) stiffness and displacement data are more meaningful as a study endpoint (presumably measuring subsidence at the level of the end plate) compared with load to failure (presumably measuring the strength of the underlying trabecular bone). Future studies will need to more closely evaluate the sequence of inciting events of implant subsidence, device migration, and end plate fracture with TDR to determine whether subsidence is a preceding event along the spectrum of injury, or if the forces needed to induce an end plate fracture are so great that the weakest link (ie, trabecular bone) fails first leaving the end plate intact [43]. A better understanding of the mechanism of failure will lead to clues as to how best to prevent these injuries (ie, implant size, patient selection, vertebral augmentation) [23].

Effects of the keel

One of the main advantages of using a keel-based TDR system is that the keel theoretically provides better fixation to the end plate than the spikes used in nonkeeled TDR devices. A more solid fixation to the surrounding bone may reduce the risk of device migration and anterior displacement that has been described [6,8,19,44,45]. It may also provide the surgeon with a visible landmark in the center of the device, which will allow for more precise midline, centered orientation. With the requisite introduction of the chisel path before TDR insertion (each of which measures 9 mm in height), followed by TDR keel placement (each of which measures 6 mm in height), there is a violation of both the superior and inferior end plates that may cause mechanical changes at the end plate [7]. This may be of particular concern for two-level TDR, where the middle vertebral body will have keel and chisel penetration of both the superior and inferior end plates [19].

Our results show that the TDR keel imparts a statistically significant reduction in end plate stiffness. For small-sized implants, the stiffness at the end plates was not significantly different when using the keeled implant (within 6%), but both the medium- and large-sized implants experienced significant decreases in end plate stiffness of 19% and 26%, respectively. However, the relevance of this mechanical alteration is not known, as in the short- to midterm follow-up there are only sparse reports of keel-related fractures and an extremely low rate of implant subsidence with the ProDisc-L [4,5,7,19,24,46]. Despite biomechanical evidence for reduced implant-explant stiffness, only long-term clinical follow-up will be able to determine whether the keel places patients at a higher risk for late complications, including end plate subsidence and fracture.

There are several study limitations inherent in a cadaveric biomechanical study. We purposely selected a broad spectrum of specimen age, bone density, and lumbar level.

Although the aged specimens would be too old for TDR surgery, eventually patients will mature to these ages and experience lower bone density. Thus, this was considered as an important factor to incorporate into the study. However, these factors increased the data variability and may have resulted in some trends that were nonsignificant. It is also possible that the mechanical properties were altered as a result of repeated testing and multiple freeze-thaw cycles; however, analysis of a subset of samples with repeated testing of the first implant size demonstrated repeatability of stiffness to within 8% and was not significantly different. Finally, although ideal disc replacement location is posterior to the center of the vertebral body, corresponding with the lumbar instantaneous axis of rotation, for this study, to avoid variable eccentric placement as a confounding variable, the specimen and indenter were aligned centrally within the middle of the vertebral body and the boundaries of the cortical rim.

In conclusion, our results support the use of the largest footplate possible to avoid large end plate displacements and reduce the potential for device subsidence and end plate failure. Likewise, device undersizing may significantly compromise the integrity of the end plate. Larger devices reduce contact forces, place the edge-loading rim on the more peripheral and stiffer vertebral body and apophyseal rim, reduce the likelihood of implant displacement, and increase the loads required to induce 2-mm displacement and fracture of the vertebral body. Bone density is highly correlated with end plate stiffness at the implant-end plate interface and is the most important factor in predicting failure loads in compression. We recommend caution in routinely using the largest TDR implant in all cases however because TDR oversizing has been described as a cause of anterior device displacement and TDR revision surgery [6,12]. Further clinical studies are needed to determine the criteria for proper TDR sizing. Finally, we have shown that the central keel of the ProDisc-L TDR implant significantly reduces the end plate stiffness by approximately 18%. These findings have clinical implications not only for proper implant sizing and insertion technique of current TDR prostheses but also for the design of future TDR systems.

Acknowledgments

References

[1] McAfee PC, Fedder IL, Saiedy S, et al. SB Charite disc replacement: report of 60 prospective randomized cases in a US center. J Spinal Disord Tech 2003;16:424–33.

[2] McAfee PC, Cunningham B, Holsapple G, et al. A prospective, randomized, multicenter Food and Drug Administration investigational device exemption study of lumbar total disc replacement with the CHARITE artificial disc versus lumbar fusion: part II: evaluation

of radiographic outcomes and correlation of surgical technique accuracy with clinical outcomes. Spine 2005;30:1576–83.

[3] Zeller JL. Artificial spinal disk superior to fusion for treating degenerative disk disease. JAMA 2006;296:2665–7.

[4] Zigler J, Delamarter R, Spivak JM, et al. Results of the prospective, randomized, multicenter Food and Drug Administration investigational device exemption study of the ProDisc-L total disc replacement versus circumferential fusion for the treatment of 1-level degenerative disc disease. Spine 2007;32:1155–62.

[5] Zigler JE, Burd TA, Vialle EN, et al. Lumbar spine arthroplasty: early results using the ProDisc II: a prospective randomized trial of arthroplasty versus fusion. J Spinal Disord Tech 2003;16:352–61.

[6] Leary SP, Regan JJ, Lanman TH, et al. Revision and explantation strategies involving the CHARITE lumbar artificial disc replacement. Spine 2007;32:1001–11.

[7] Shim CS, Lee S, Maeng DH, et al. Vertical split fracture of the vertebral body following total disc replacement using ProDisc: report of two cases. J Spinal Disord Tech 2005;18:465–9.

[8] van OA, Oner FC, Verbout AJ. Complications of artificial disc replacement: a report of 27 patients with the SB Charite disc. J Spinal Disord Tech 2003;16:369–83.

[9] van OA, Schurink GW, Oner FC, et al. Findings in 67 patients with recurrent or persistent symptoms after implantation of a disc prosthesis for low back pain. Ned Tijdschr Geneeskd 2007;151:1577–84.

[10] van OA, Kurtz SM, Stessels F, et al. Polyethylene wear debris and long-term clinical failure of the Charite disc prosthesis: a study of 4 patients. Spine 2007;32:223–9.

[11] Wagner WH, Regan JJ, Leary SP, et al. Access strategies for revision or explantation of the Charite lumbar artificial disc replacement. J Vasc Surg 2006;44:1266–72.

[12] Cinotti G, David T, Postacchini F. Results of disc prosthesis after a minimum follow-up period of 2 years. Spine 1996;21:995–1000.

[13] Zeegers WS, Bohnen LM, Laaper M, et al. Artificial disc replacement with the modular type SB Charite III: 2-year results in 50 prospectively studied patients. Eur Spine J 1999;8:210–7.

[14] Kurtz SM, van OA, Ross R, et al. Polyethylene wear and rim fracture in total disc arthroplasty. Spine J 2007;7:12–21.

[15] Oxland TR, Grant JP, Dvorak MF, et al. Effects of endplate removal on the structural properties of the lower lumbar vertebral bodies. Spine 2003;28:771–7.

[16] Hasegawa K, Abe M, Washio T, et al. An experimental study on the interface strength between titanium mesh cage and vertebra in reference to vertebral bone mineral density. Spine 2001;26:957–63.

[17] Lowe TG, Hashim S, Wilson LA, et al. A biomechanical study of regional endplate strength and cage morphology as it relates to structural interbody support. Spine 2004;29:2389–94.

[18] Tan JS, Bailey CS, Dvorak MF, et al. Interbody device shape and size are important to strengthen the vertebra-implant interface. Spine 2005;30:638–44.

[19] Stieber JR, Donald GD III. Early failure of lumbar disc replacement: case report and review of the literature. J Spinal Disord Tech 2006;19:55–60.

[20] Higgins KB, Harten RD, Langrana NA, et al. Biomechanical effects of unipedicular vertebroplasty on intact vertebrae. Spine 2003;28:1540–7.

[21] O'Connell GD, Vresilovic EJ, Elliott DM. Comparison of animals used in disc research to human lumbar disc geometry. Spine 2007;32:328–33.

[22] Panjabi MM, Goel V, Oxland T, et al. Human lumbar vertebrae. Quantitative three-dimensional anatomy. Spine 1992;17:299–306.

[23] Auerbach JD, Yoder HY, Maurer PM, et al. Vertebral body augmentation with Cortoss improves compression biomechanics for lumbar disc arthroplasty. Proceedings of the 34th International Society for the Study of the Lumbar Spine Annual Meeting, Hong Kong, 151. 2007. [Ref Type: Abstract].

[24] Delamarter RB, Bae HW, Pradhan BB. Clinical results of ProDisc-II lumbar total disc replacement: report from the United States clinical trial. Orthop Clin North Am 2005;36:301–13.

[25] Auerbach JD, Wills BP, McIntosh TC, et al. Evaluation of spinal kinematics following lumbar total disc replacement and circumferential fusion using in vivo fluoroscopy. Spine 2007;32:527–36.

[26] Cunningham BW, Gordon JD, Dmitriev AE, et al. Biomechanical evaluation of total disc replacement arthroplasty: an in vitro human cadaveric model. Spine 2003;28:S110–7.

[27] Dmitriev AE, Cunningham BW, Hu N, et al. Adjacent level intradiscal pressure and segmental kinematics following a cervical total disc arthroplasty: an in vitro human cadaveric model. Spine 2005;30:1165–72.

[28] Ghiselli G, Wang JC, Bhatia NN, et al. Adjacent segment degeneration in the lumbar spine. J Bone Joint Surg Am 2004;86-A:1497–503.

[29] Gillet P. The fate of the adjacent motion segments after lumbar fusion. J Spinal Disord Tech 2003;16:338–45.

[30] Lai PL, Chen LH, Niu CC, et al. Relation between laminectomy and development of adjacent segment instability after lumbar fusion with pedicle fixation. Spine 2004;29:2527–32.

[31] Lee CK. Accelerated degeneration of the segment adjacent to a lumbar fusion. Spine 1988;13:375–7.

[32] Park P, Garton HJ, Gala VC, et al. Adjacent segment disease after lumbar or lumbosacral fusion: review of the literature. Spine 2004;29:1938–44.

[33] Quinnell RC, Stockdale HR. Some experimental observations of the influence of a single lumbar floating fusion on the remaining lumbar spine. Spine 1981;6:263–7.

[34] Shono Y, Kaneda K, Abumi K, et al. Stability of posterior spinal instrumentation and its effects on adjacent motion segments in the lumbosacral spine. Spine 1998;23:1550–8.

[35] Weinhoffer SL, Guyer RD, Herbert M, et al. Intradiscal pressure measurements above an instrumented fusion. A cadaveric study. Spine 1995;20:526–31.

[36] Huang RC, Lim MR, Girardi FP, et al. The prevalence of contraindications to total disc replacement in a cohort of lumbar surgical patients. Spine 2004;29:2538–41.

[37] Wong DA, Annesser B, Birney T, et al. Incidence of contraindications to total disc arthroplasty: a retrospective review of 100 consecutive fusion patients with a specific analysis of facet arthrosis. Spine J 2007;7:5–11.

[38] David T. Long-term results of one-level lumbar arthroplasty: minimum 10-year follow-up of the CHARITE artificial disc in 106 patients. Spine 2007;32:661–6.

[39] Labrom RD, Tan JS, Reilly CW, et al. The effect of interbody cage positioning on lumbosacral vertebral endplate failure in compression. Spine 2005;30:E556–61.

[40] Polikeit A, Ferguson SJ, Nolte LP, et al. Factors influencing stresses in the lumbar spine after the insertion of intervertebral cages: finite element analysis. Eur Spine J 2003;12:413–20.

[41] Siepe CJ, Wiechert K, Khattab MF, et al. Total lumbar disc replacement in athletes: clinical results, return to sport and athletic performance. Eur Spine J 2007;16:1001–13.

[42] Kayanja MM, Schlenk R, Togawa D, et al. The biomechanics of 1, 2, and 3 levels of vertebral augmentation with polymethylmethacrylate in multilevel spinal segments. Spine 2006;31:769–74.

[43] Ochia RS, Tencer AF, Ching RP. Effect of loading rate on endplate and vertebral body strength in human lumbar vertebrae. J Biomech 2003;36:1875–81.

[44] Caspi I, Levinkopf M, Nerubay J. Results of lumbar disk prosthesis after a follow-up period of 48 months. Isr Med Assoc J 2003;5:9–11.

[45] Griffith SL, Shelokov AP, Buttner-Janz K, et al. A multicenter retrospective study of the clinical results of the LINK SB Charite intervertebral prosthesis. The initial European experience. Spine 1994;19:1842–9.

[46] Tropiano P, Huang RC, Girardi FP, et al. Lumbar total disc replacement. Seven to eleven-year follow-up. J Bone Joint Surg Am 2005;87:490–6.